AIP | Review of Scientific Instruments

Core-ion temperature measurement of the ADITYA tokamak using passive charge exchange neutral particle energy analyzer

Santosh P. Pandya, Kumar Ajay, Priyanka Mishra, Rajani D. Dhingra, and J. Govindarajan

Citation: Review of Scientific Instruments **84**, 023503 (2013); doi: 10.1063/1.4791998
View online: http://dx.doi.org/10.1063/1.4791998
View Table of Contents: http://scitation.aip.org/content/aip/journal/rsi/84/2?ver=pdfcov
Published by the AIP Publishing

Core-ion temperature measurement of the ADITYA tokamak using passive charge exchange neutral particle energy analyzer

Santosh P. Pandya, Kumar Ajay,[a] Priyanka Mishra,[b] Rajani D. Dhingra,[b] and J. Govindarajan
Institute for Plasma Research, Bhat, Gandhinagar 382 428, Gujarat, India

(Received 23 October 2012; accepted 29 January 2013; published online 20 February 2013)

Core-ion temperature measurements have been carried out by the energy analysis of passive charge exchange (CX) neutrals escaping out of the ADITYA tokamak plasma (minor radius, $a = 25$ cm and major radius, $R = 75$ cm) using a 45° parallel plate electrostatic energy analyzer. The neutral particle analyzer (NPA) uses a gas cell configuration for re-ionizing the CX-neutrals and channel electron multipliers (CEMs) as detectors. Energy calibration of the NPA has been carried out using ion-source and $\Delta E/E$ of high-energy channel has been found to be ~10%. Low signal to noise ratio (SNR) due to VUV reflections on the CEMs was identified during the operation of the NPA with ADITYA plasma discharges. This problem was rectified by upgrading the system by incorporating the additional components and arrangements to suppress VUV radiations and improve its VUV rejection capabilities. The noise rejection capability of the NPA was experimentally confirmed using a standard UV-source and also during the plasma discharges to get an adequate SNR (>30) at the energy channels. Core-ion temperature $T_i(0)$ during flattop of the plasma current has been measured to be up to 150 eV during ohmically heated plasma discharges which is nearly 40% of the average core-electron temperature (typically $T_e(0) \sim 400$ eV). The present paper describes the principle of tokamak ion temperature measurement, NPA's design, development, and calibration along with the modifications carried out for minimizing the interference of plasma radiations in the CX-spectrum. Performance of the NPA during plasma discharges and experimental results on the measurement of ion-temperature have also been reported here. © *2013 American Institute of Physics*. [http://dx.doi.org/10.1063/1.4791998]

I. INTRODUCTION

Ion temperature in hot plasmas may be measured by several well developed methods,[1–7] each having its advantages and disadvantages. Ion temperature measurement methods based on the monitoring of charge exchange (CX) neutrals are well established techniques.[7–23] A convenient method is to obtain CX-neutral mass/energy resolved spectra using electromagnetic field.[9–19] Energetic neutral particles that are formed due to charge exchange of plasma ions with neutral atoms escape the plasma readily since neutral do not interact with electric or magnetic fields of tokamaks. These neutral atoms which are re-ionized and analyzed give the information about the plasma ion energy distribution. Even though this method has some limitations, the ion temperature estimate obtained is fairly accurate. The method is applied to the ADITYA tokamak for ion-temperature measurements.

The ADITYA is the first indigenously designed and built tokamak of the country.[24,25] It is a medium size tokamak, having major radius (R) of 75 cm and minor radius of the plasma (a) is 25 cm. A maximum of 1.2 T toroidal magnetic field (B_T) is generated with the help of 20 toroidal field coils spaced symmetrically in the toroidal direction. The major subsystems and parameters of the machine have been described in Refs. 24 and 25. The typical plasma parameters during plasma discharges are: plasma current (I_p) ~ 70–100 kA, hydrogen plasma discharge duration ~80–100 ms, central electron temperature ($T_e(0)$) ~ 300–400 eV, core plasma density ($N_e(0)$) ~ 1–3 × 10^{13} cm^{-3}, and input ohmic power ~200 kW.

In the ADITYA tokamak, having hydrogen plasma discharge, the hot plasma is confined inside the circular limiter. The region between the plasma and the tokamak walls is filled with hydrogen gas at the wall temperature. The hydrogen molecules get dissociated and ionized as they diffuse into the hot plasma (Franck–Condon neutrals).[7] Thus, the density of neutral atoms falls rapidly towards the core of the plasma. These neutral atoms undergo resonant charge exchange interaction of type

$$H^+_{hot} + H^0_{cold} \rightarrow H^0_{hot} + H^+_{cold}.$$

The number of such fast neutrals produced depends on the energy and density of the plasma particles, density of neutrals atoms, and the reaction rates. All the fast neutrals produced inside the plasma do not reach the detectors. Some of them encounter interactions within the plasma and some reflect inside by hitting the walls. The secondary interactions act as attenuation to the fast CX-neutrals. The mean free path λ_{cx} of such interactions is a function of plasma density n, the reaction cross section σ (which in turn depends on the energy of CX-neutral), and is given by

$$\lambda_{cx} = \frac{1}{n\sigma(E)}. \quad (1)$$

[a]Author to whom correspondence should be addressed. Electronic mail: ajaykuma@ipr.res.in. Tel.: +91-79-23962182. Fax: +91-79-23962277.
[b]This research was performed while author was at Institute for Plasma Research, Bhat, Gandhinagar 382 428, Gujarat, India.

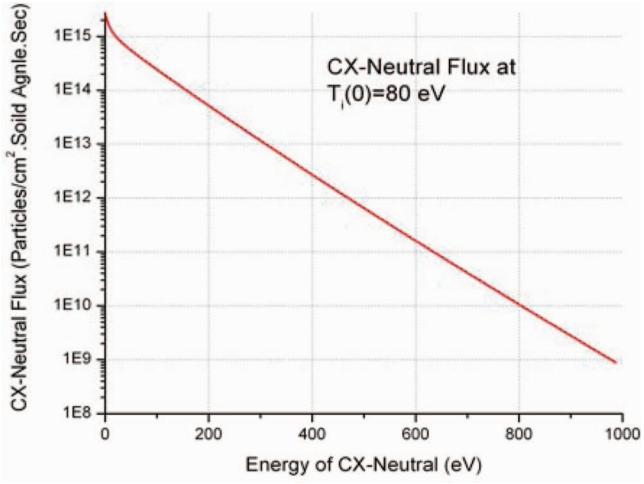

FIG. 1. Calculated CX-neutral energy spectrum for ADITYA tokamak. The results have been obtained analytically using the slab-model assumption for ohmic plasma's circular cross section.

As the size and density of the plasma is increased the neutrals formed at the plasma center and towards the inboard side of the tokamak get attenuated and their probabilities to reach the neutral particle analyzer (NPA) detector become very low. As a consequence, the energy distribution measured is from the shallow depths from the edge. In short, the applicability of such neutral analysis is limited for plasmas with $\int n(r)\,dr$ to be less than 10^{13} cm^2 or a few times more where $n(r)$ is the ion density as a function of position r and integration is over the distance, the fast neutral particle has to travel inside the plasma up to the edge in the direction of the detector without undergoing any secondary collisions.

Brief description of the NPA is presented in Sec. II, principle of ion temperature measurement is described in Sec. III, possible errors in the ion temperature measurements have been explained in Sec. IV, while energy calibration and related results are described in Sec. V. In Sec. VI, the experimental observations of VUV noise, systematic modification in the NPA for the suppression of VUV noise, and testing of NPA during ADITYA plasma discharge are presented. Estimation of ion temperature during ohmic plasma discharges has been discussed in Sec. VII.

II. DESCRIPTION OF THE CX-NPA SYSTEM

CX-neutral flux has been estimated using the slab-theory model,[7,26] assuming the parabola profile of density and temperature. A charge exchange flux vs energy distribution, using this model (with a typical values of core ion temperature T_i (0) ~80 eV and average plasma density is $\langle n \rangle \sim 1.5 \times 10^{13}$ cm^{-3}) has been shown in Fig. 1. Considering the minimum and maximum energy of CX-neutrals, the 45° parallel plate electrostatic energy analyzer is designed for the ADITYA tokamak.[9–12,27,28]

A layout of the ADITYA charge exchange diagnostic system has been shown in Fig. 2, which is connected to the tokamak's radial port no. 10 through frustum. Detailed description of the NPA is given in Ref. 28. The present NPA utilizes gas cell configuration for the stripping of CX-neutrals and this configuration is preferred instead of thin carbon foil configuration because of low energies expected, as seen in Fig. 3. The stripping cell is a 20 cm long narrow tube of diameter 0.4 cm, made of soft iron in order to decrease the fringing field effects on the stripped CX-neutrals (re-ionized CX-neutrals). During operation the cell is filled with H_2 gas and maintained at a pressure of 5 mtorr for getting an optimum efficiency of the stripping reaction with the given energy range of the CX-neutrals (typically from 100 eV to 1 keV). The stripping cell is differentially pumped by the pumping line. The analyzer box is a vacuum chamber made of 2.5 cm thick soft iron plates. Plate thickness is optimized to minimize the magnetic field effect during the plasma discharges.[9,28]

The tokamak's magnetic field near the analyzer box is $B_{out} \sim 100$ Gauss. However, the minimized magnetic field effect (due to the shielding of the box by soft iron plates) during the plasma discharge is given by

$$B_{in} = B_{out}\frac{3r}{5\mu t}. \tag{2}$$

The vessel reduces the stray magnetic field, i.e., B_{in} down to ~0.03 Gauss in the present case. The parallel plate analyzer is placed at 45° close to stripping gas cell for a better energy resolution.[9–12,27] Channel electron multipliers (CEM, Amptektron make, Model MD-501) are used to detect the particles.[29] The whole system is pumped down to a pressure of $\sim 2 \times 10^{-6}$ torr by a 1100 l/s turbo molecular pump

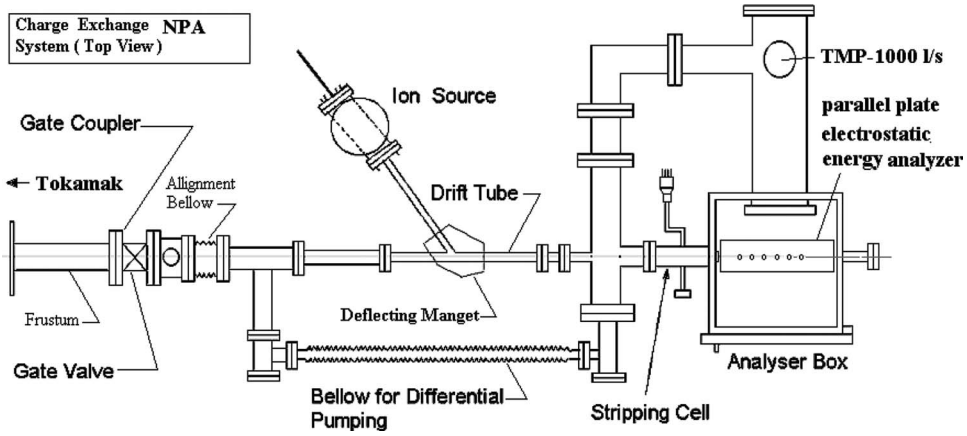

FIG. 2. Schematic layout of the ADITYA charge exchange NPA.

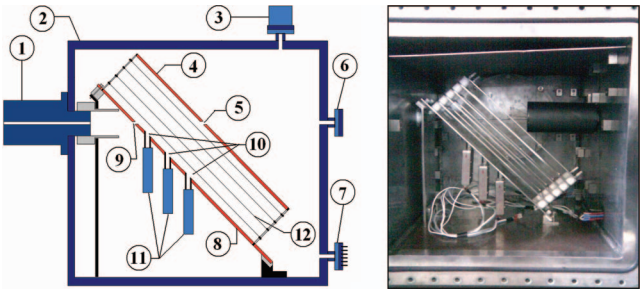

FIG. 3. Schematic layout of the CX-NPA and its photograph. Components inside CX-NPA are (1) stripping cell, (2) analyzer box, (3) pressure gauge, (4) positive plate (PP), (5) exit aperture at PP (straight channel), (6) alignment window, (7) electrical feedthrough, (8) grounded plate (GP), (9) entrance aperture, (10) exit apertures at GP (energy channels), (11) CEM-detector, (12) guard rings.

(Oerlikon Leybold make, Model: TURBOVAC 1100 C). The main gas load comes from the stripping gas cell. The viewing geometry of the analyzer has been chosen such that it samples ±0.5 cm vertically and ±1.0 cm toroidally at the plasma center. The solid angle subtended by the plasma at the stripping cell is $\Omega \sim 10^{-6}$ steradians.

III. PRINCIPLE OF ION TEMPERATURE ESTIMATION

The charged particles under the influence of a retarding field follow a parabolic path and go back to the plate PG at a distance X from the entrance point. This range X is given by[9–12,27]

$$X = \frac{2Ed}{V_p}, \tag{3}$$

where d is the distance between the plates PG and PP, i.e., 10 cm in present case, E is the energy of the incident particle in eV, and V_p is the voltage applied to the analyzer plates. Thus, the particle going out through exit holes at a distance X_i would have an energy given by

$$E_i = \frac{V_p}{2d} X_i. \tag{4}$$

Since the entrance angle θ is too small ($<1^{\circ}$) for the ions entering into the analyzer even after experience scattering in stripping cell,[10] the energy resolution is given by[9–12,27]

$$\frac{\Delta E_i}{E} = \frac{(\Delta X_0 + \Delta X_i)}{X_i}, \tag{5}$$

where ΔX_0 is the width of the entrance aperture (0.65 cm) and ΔX_i is the width of the exit aperture or the detector aperture (0.65 cm). It should be noted that as the range X_i reduces, the energy resolution gets deteriorated.

The number of counts recorded at the exit of the analyzer corresponding to the ion's energy E is given by

$$C(E) = \frac{\Omega}{4\pi} \eta_s \eta_t \eta_c N(E) \Delta E \Delta t, \tag{6}$$

where Δt is the time interval over which counts are collected, Ω is the solid angle subtended by the stripping cell at the plasma center, η_s is the stripping cell efficiency, η_t is the net transmission efficiency, η_c is the detection efficiency of the CEM, ΔE is the energy resolution of the analyzer, and $N(E) \cdot \Delta E$ is the number of neutrals in the energy range $E + \Delta E$ emitted per second from the volume ΔV sampled by the analyzer which can further be represented as

$$N(E) = \Delta V \eta_0 \eta_+ f \sigma_{cx} v, \tag{7}$$

where η_0 and η_+ are the neutral and ion densities, respectively, σ_{cx} is the cross section for the CX reaction at ion energy E, v is the relative velocity between neutrals and ion undergoing charge exchange, and f is the Maxwellian distribution function given by

$$f = \frac{2}{T}\sqrt{\frac{E}{\pi T}} \exp^{-E/T}, \tag{8}$$

where T is the ion temperature and the isotropic velocity distribution of the ions has been assumed.

Substituting Eqs. (7) and (8) in Eq. (6) we get the expression for the counts $C(E)$ at a channel with energy E as

$$C(E) = \frac{\Omega}{4\pi} \Delta V \eta_s \eta_t \eta_c \eta_0 \eta_+ \frac{2}{T}\sqrt{\frac{E}{\pi T}} \exp^{-E/T} \Delta E \sigma_{cx} v \Delta t. \tag{9}$$

Factoring out the energy dependent terms we get

$$\ln F = \ln K - \frac{E}{T}, \tag{10}$$

$$\text{where } \boldsymbol{F} \text{ is } \quad \frac{C(E)}{\eta_s \sigma_{cx} v \sqrt{E} \Delta E} \tag{11}$$

and $\boldsymbol{K}$ is

$$\frac{\Omega}{4\pi} \Delta V \eta_s \eta_t \eta_c \eta_0 \eta_+ \frac{2}{T}\sqrt{\frac{1}{\pi T}} \Delta t. \tag{12}$$

So knowing the energy dependent quantities in F (η_s, $\langle \sigma_{cx} v \rangle$, ΔE, and C (E) at different E) one can obtain the inverse of the slope given by Eq. (10) as an estimate of the core ion temperature.

However, the plot obtained by Eq. (10) will deviate from a straight line at lower energies because the plasma temperature is not constant along the line of sight. It peaks in the center and falls off parabolically towards the walls. Further, low energy charge exchange neutrals emitted from the center of the plasma would be attenuated as they travel through the rest of the plasma. Because of these two effects, the experimental data would slightly deviate from the straight line given by Eq. (10). To overcome this problem, only that portion of the curve having range $2T_i$ (0) $< E < 7T_i$ (0) is conventionally used for the core-ion temperature estimation,[2,9,30–33] since attenuation is less for higher energy neutrals and contribution to energetic neutrals is less from the outer region of the plasma. In the present paper, measurements were carried out between $3T_i$ (0) $< E < 5T_i$ (0), because for $E \geq 5T_i$ (0) there were not enough detected particles and high stray VUV reflections at higher energy channels.

IV. ERRORS IN THE ION TEMPERATURE ESTIMATION

Underestimation in the ion temperature measurement by the above technique can be overcome by taking the slope of

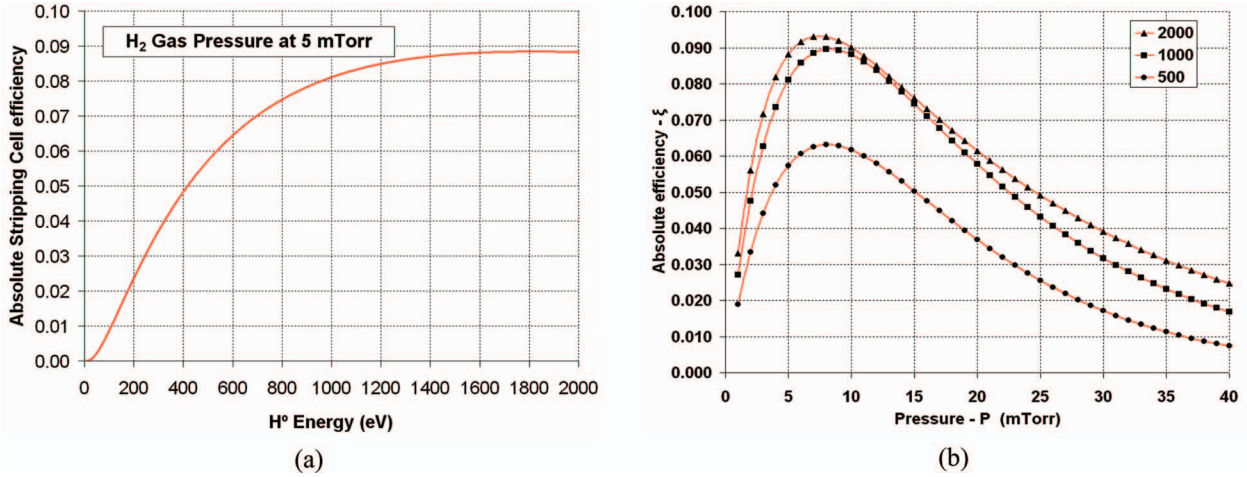

FIG. 4. (a) Stripping efficiency as a function of neutral energy (E) in eV. (b) Stripping cell efficiency as a function of H2 gas pressure in mtorr. [Refer to Eq. (13).]

the straight line represented by Eq. (10) in the higher energy region to ensure that we are monitoring the Maxwellian contributed solely by the core region of the plasma.[9,30–33]

Another source of errors can be from the inaccuracies of the measurements done in getting the stripping cell efficiency. Major uncertainties in the stripping cell efficiencies are because of the errors in the various cross sections involved and the stripping cell pressure. The cross section issues can be eliminated by determining the stripping cell efficiency experimentally.[10] However, the pressure variations (minor fluctuations) during the experiments are inevitable. This is because at low energies stripping cell efficiency is very sensitive to even small changes in the pressure of the cell.

The efficiency of the stripping cell being used in the ADITYA charge exchange NPA system can be given by[9,10,16]

$$\eta_s = \frac{\sigma_{01}}{(\sigma_{01}+\sigma_{10})}\exp^{-(\alpha\sigma_s)}\{1-\exp^{(-\alpha|\sigma_{01}+\sigma_{10}|)}\}, \tag{13}$$

where $\alpha = \frac{lC_1p}{2}$ and $\sigma_s = \frac{F_s\times10^{-16}}{E^{1/2}}$, the scattering cross section, and E is the energy of particle in keV. F_s is a fitting parameter. $C_1 = \frac{\rho_{Hg}\times g\times10^4}{KT}$, with p being the pressure in mtorr, l is the length of the cell in cm, K is the Boltzmann constant in erg/degree K, g is the acceleration due to gravity in cm/s^2, ρ_{Hg} is the density of mercury in gm/cm^3, and C_1 is equal to 3.23 $\times$ 10^{13}. The stripping cell efficiency as a function of neutral energy is given in Fig. 4(a) and variation of efficiency with gas pressure is plotted in Fig. 4(b). So it can be shown that

$$\frac{\Delta\eta}{\eta} = \frac{\Delta p}{p}\left[-K_1 + \frac{K_2}{\exp^{K_2p}-1}\right], \tag{14}$$

where K_1 is $\frac{lc_1\sigma_S}{2}$ and K_2 is $\frac{lC_1(\sigma_{01}+\sigma_{10})}{2}$. The quantity $\xi = |\frac{\Delta\eta/\eta}{\Delta p/p}|$ is called sensitivity. The other sources in the temperature measurements error are the statistical error in counts at a particular channel $\Delta C(E)/C(E)$, error due to energy broadening $\Delta E/E$, and the error in the data for the charge exchange cross section at energy E, i.e., $\Delta\sigma_{cx}/\sigma_{cx}$. So the overall error in T_i will be

$$\frac{\Delta T_i}{T_i} = \frac{\Delta S}{S}, \tag{15}$$

where S is the slope given by Eq. (10) and ΔS represents the error in this slope. Error in the slope ΔS will depend on error in ln$F$ given by

$$\Delta\ln F = \sqrt{\left(\left(\frac{\Delta C(E)}{C(E)}\right)^2 + \left(\frac{\Delta\eta}{\eta}\right)^2 + \left(\frac{\Delta E}{E}\right)^2 + \left(\frac{\Delta\sigma}{\sigma}\right)^2\right)}. \tag{16}$$

V. ENERGY CALIBRATION OF CX-NPA

The CX-NPA was calibrated for different analyzer plate voltages and corresponding energies focused at three different energy channels using a H^+ ion source. Low energy beam (100 to 1000 eV) of hydrogen ions is produced by plasma discharge based ion source. H^+ beam of the desired energy is produced in continuous mode having a beam current of $\sim$1 μA to 5 μA. The beam is allowed to pass through the stripping cell (without gas) and thereafter it enters into the parallel plate analyzer from the input slit. The retarding analyzer plate voltage is varied and tuned such that the hydrogen beam of particular energy will focus on different specific energy channels one by one. Count rates on each channel are recorded as a function of applied plate voltage and the voltage at peak value of the counts is considered as corresponding focusing voltage for that beam energy. Figure 5 shows typical example for beam energy of 100 to 600 eV focused at the energy channel-2 by sweeping the analyzer plate voltage from 0 to 2000 V.

The relation between the analyzer plate voltage V_p and corresponding focusing different energies on three energy channels is shown in Figs. 5 and 6.

By measuring the FWHM of the different count peaks for three energy channels $\Delta E/E$ for each channel is calculated. Table I shows the calculated and experimental values of $\Delta E/E$

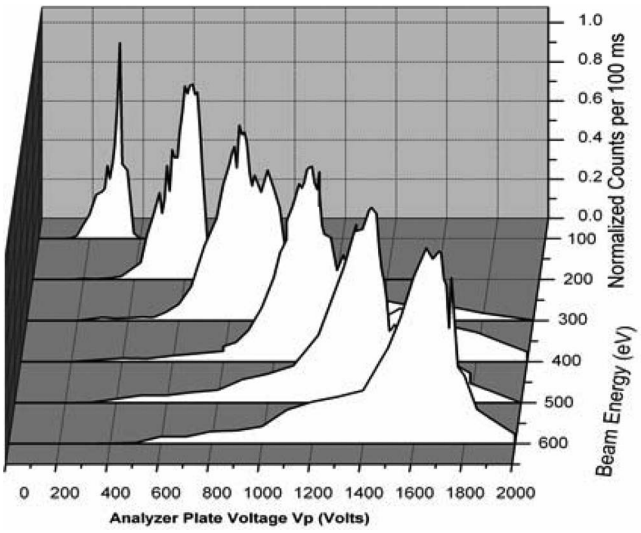

FIG. 5. Different count peaks correspond to different analyzer plate voltage Vp and H^+ beam energy for channel-2.

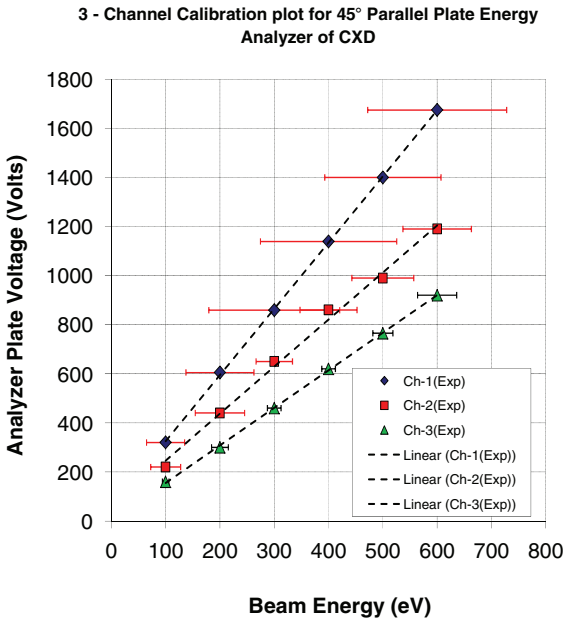

FIG. 6. CX-NPA calibration curve analyzer plate voltage (Vp) vs detected energy (E) for three different channels. [Refer to Eq. (3).]

for 500 eV beam. As per the experimental values given in the table, we are not in a very good agreement with the calculated values and this can be attributed to the presence of the ion species other than H^+ in the ion source beam.

VI. RESULTS AND DISCUSSIONS

A. Interference of VUV in charge exchange neutral's spectrum and its suppression

As the ACX-NPA was operated during plasma shots, spurious counts of the order $\sim 10^4$ at 10 ms (expected counts $\sim$50 to a few hundreds at 10 ms) at the channels were recorded. We would, in brief, describe the observations and the conclusion as below:

1. No signal was observed during vacuum shots with or without gate valve open.
2. There were no signals during a plasma shot ON with gate valve closed.
3. There was no spurious signal observed during calibration of energy channels.
4. Interchanging the electrical connections of the CEMs did not affect the count on a particular channel.
5. No counts were seen with plasma shot having full hard x rays.
6. Those noisy counts disappeared when the detector opening was shielded with teflon tape.

All the above observations clearly ruled out the role of any grounding problem or picking up of stray signals.

7. The noisy counts were observed only during plasma shot with gate valve open.
8. No remarkable effect of pressure variation in stripping cell was observed on these counts.
9. There was no change in counts with or without electrical field of plates and the reversal of the same.

CEMs are sensitive to charge particles, soft x rays, and VUV radiations only (Fig. 7).[29] The possibility of charge particles was ruled out with the help of observations in serial no. 8 and 9. Again, the possibility of secondary electrons being detected by the CEM was also ruled out as the detector was set in the ion selection mode. Chances of soft x rays to be reflected back and to be detected on CEMs are almost rare, because 225 Å is the minimum-reflecting wavelength from the well polished analyzer-wall at normal incidence. So the possibilities of stray VUV photons being reflected from the inner walls of stripping cell as well as the analyzer plates and falling back on the CEMs were there. The counts generated by the CEMs because of this came out to be the main contributors to the spurious counts.

Inspired by a survey of several tokamaks regarding radiation suppression and shielding in NPAs,[10–19] we tried to

TABLE I. Table of the three energy channels and corresponding energy resolutions.

Channel no.	Distance of detector aperture from striping cell (exit slit) center X_i (cm)	Energy resolution $\Delta E/E$ Corresponding to $E = 500$ eV beam energy	
		Calculated $\frac{\Delta E_i}{E} = \frac{(\Delta X_0 + \Delta X_i)}{X_i}$	Experimental value of $\frac{\Delta E_i}{E} = \frac{\text{FWHM of Peak}}{E}$
1	7.0	0.20	0.41
2	10.5	0.13	0.22
3	14.0	0.10	0.12

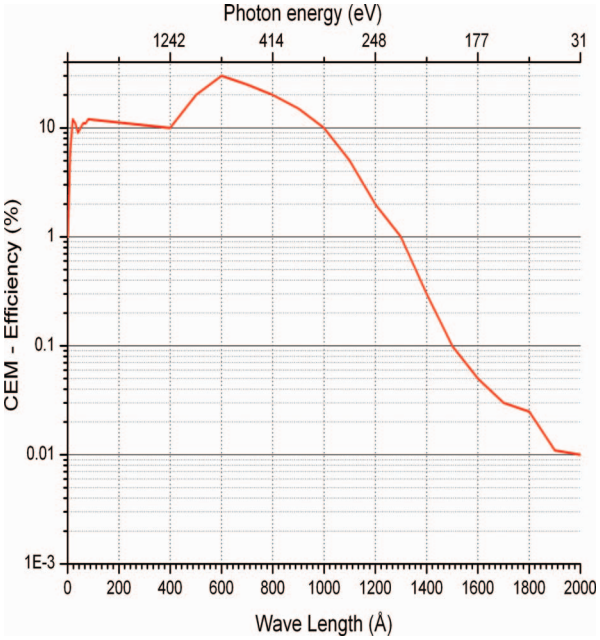

FIG. 7. CEM photon detection efficiency with wavelength.[29]

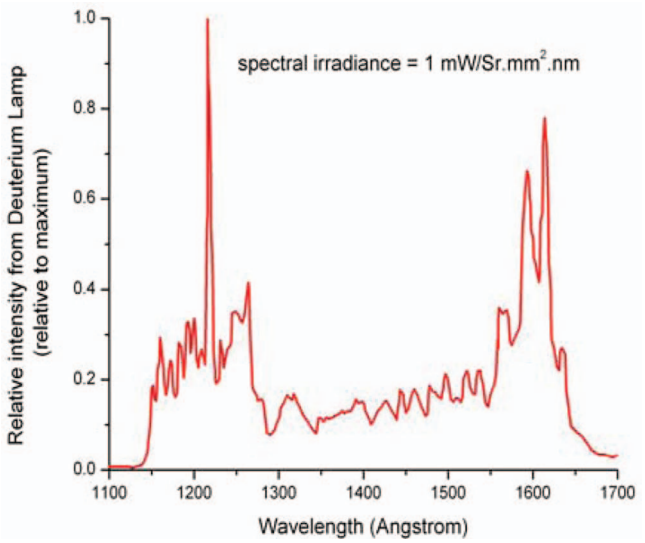

FIG. 9. Deuterium lamp's spectrum used to test the UV rejection capabilities of the upgraded ACX-NPA.

solve the problem of unwanted counts due to radiations in the ACX-NPA by doing some modifications. The schematic of the modified system can be viewed as in Fig. 8. Modifications were done in the ACX-NPA to suppress the radiative noise. The modified and the additional components incorporated in the ADITYA charge exchange system can be summarized as below:

1. The tube connecting the frustum to the analyzer box consists of baffles coated with Xylan® black paint to prevent the UV radiations from plasma.
2. Such collimating arrangements have also been incorporated between the stripping cell and the entrance of analyzer.
3. There is an additional collimating unit at the exit of the electrostatic plate PP.
4. A radiation dump has been set at the straight channel (which is in the line of the ion beam and at the rear of the analyzer box) to stop the back streaming of the radiation.
5. The internal surface of parallel plates and other internal components are coated with Xylan® black paint.
6. The soft iron vessel has been coated with black Xylan® paint. Xylan® has an excellent vacuum compatibility up to 10^{-6} Torr.

The charge exchange system along with and without the aforesaid updated configuration was tested and the results were compared for its VUV reflections using a deuterium lamp (Model DS-775, ACTON RESEARCH CORPORATION, US). The intensity distribution of various wavelengths emitted by this deuterium-lamp has been given in Fig. 9.

The results of the experiments which have been conducted to measure the suppression of VUV reflections at the energy channels (CEMs) are presented in Table. II. This was done for channel-3, where comparatively a high reflection of UV is expected.

The overall suppression of the spurious background counts after the incorporation of additional components was up to 100% (UV rejection factor $>10^{-5}$). The added components thus aided in the drastic minimization of the radiative reflection on the channels. The calibration mentioned in Sec. V which was carried out after all these modifications that depict the functionality of the NPA is not changed.

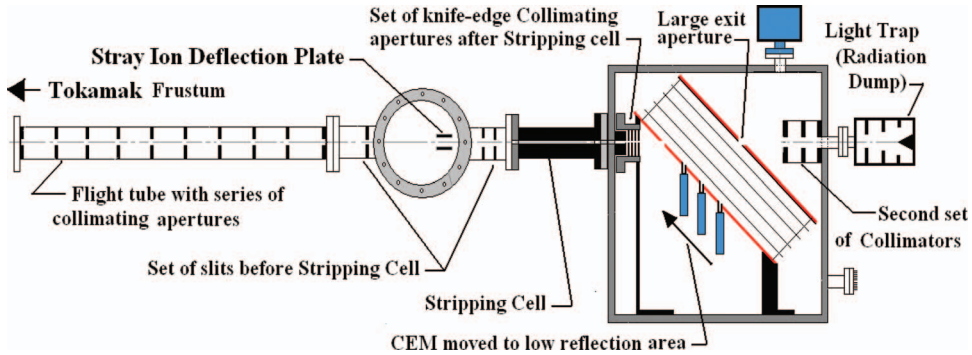

FIG. 8. Side view of the CX-NPA after modifications made for the UV suppression.

TABLE II. The suppression of VUV photons as seen on Channel-3 after the incorporation of additional components in the ACXD System.

Sr. no.	Name of the components/modifications steps	Typical VUV counts per 1 s at Channel-3	Suppression of VUV counts (Relative to base counts in %)
1	Base counts – previous configuration (No components/No modification in the ADITYA CX-NPA system)	77 187	00.00
2	Coating of the Xylan® black paint on inner surface of the positive plate that decreases reflection of VUV photons	11 699	84.84
3	A thorough hole in the positive plate at straight channel having 0.6 cm diameter which passes most of the VUV photons and minimizes reflection. In this configuration Xylan® black paint is not coated on inner surface of the positive plate (Sr. No. 2)	4480	94.20
4	Combination of both above mentioned configurations (Sr. No.: 2 and 3) that is through hole and black paint coating	1116	98.55
5	With configuration in Sr. No. 4, the through-hole diameter is increased about 1.0 cm and fine conducting tungsten mesh is placed on the through hole to prevent electric filed distortion.	303	99.61
6	Placing of additional baffle before stripping gas cell and collimating aperture in flight tube	167	99.78
7	Radiation-dump and light gathering cylinder (2nd set of collimators)	22	99.97
8	Internal coating of the CEM detector connecting tube	11	99.99
9	Knife edge collimating apertures between stripping-cell and entrance aperture of detector grounding plate (GP)	6	99.99
10	Detectors shifted to low VUV reflection region (Fig. 8)	0	100.00

B. Testing of NPA with ADITYA plasma discharges

The summary of the observations after the upgradations of system has been illustrated in Fig. 10. The observations were as below:

1. The background level of counts [dark level in present case] came down to ∼10 to 20 counts (per 10 ms).
2. The charge exchange signal strength remarkably increased when the gas cell was filled with hydrogen at an optimum pressure [∼5 mtorr].
3. The channels received only the dark background (as mentioned in point-1) counts after the stripping cell gas was put off.
4. The charge exchange signal disappeared by applying a negative plate voltage or by withdrawing the positive voltage at analyzer plate. This along with the observation number 3 above confirms the detected signal to be only the CX-neutrals.

VII. ESTIMATION OF ION TEMPERATURE DURING OHMIC HEATING

The estimation of ion temperature with ADITYA plasma discharge number 21 744 has been illustrated (Figs. 11–13). Least square fitting of the straight line obtained by the plot of ln$F$ vs energy was done (Fig. 12) and then the temperature was estimated. The ion temperature for ADITYA plasma has been presented here at a time resolution of 15 ms during flat-tops of plasma current I_p (Fig. 13) which sustains typically for 100 ms to 120 ms.

Figure 14 shows the temporal evolution of electron temperature during ohmic heating and its evolution has been compared with the core ion temperature obtained using ACX-NPA. It has been found that the peak ion temperature is typically 40% to 45% of the central electron temperature.

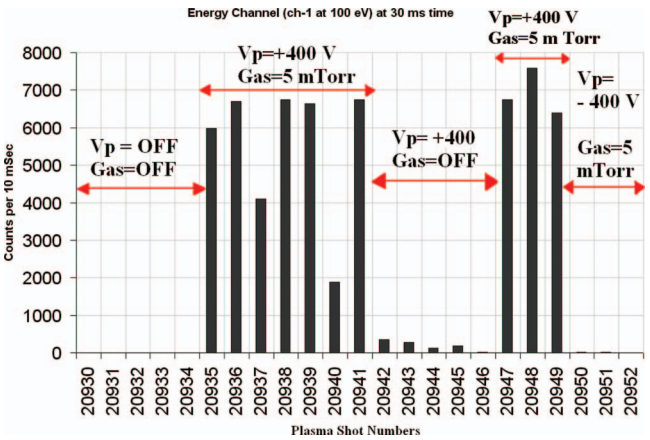

FIG. 10. The illustration of charge exchange neutrals generated signals at CEM after filling up hydrogen gas at 5 mTorr in the stripping cell.

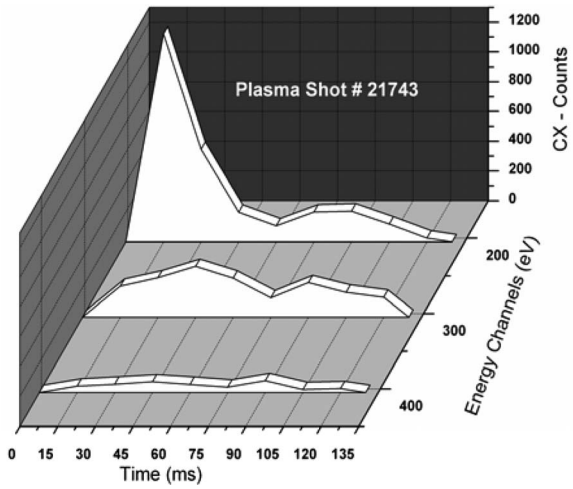

FIG. 11. Plot shows CX-neutral counts at three different energy channels with time.

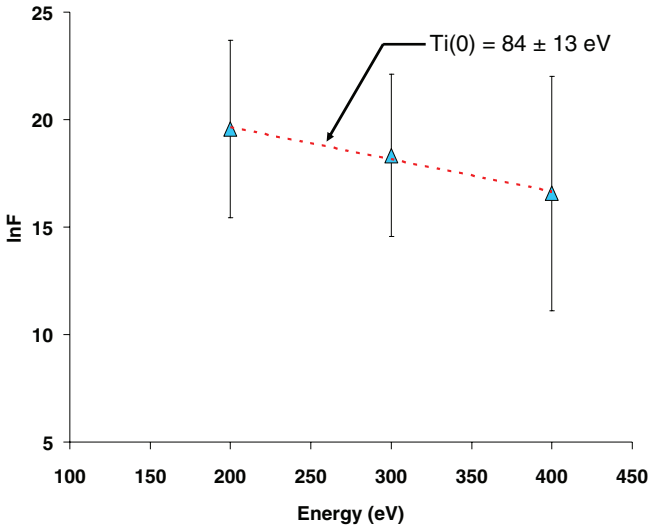

FIG. 12. Plot of ln$F$ vs counts at various energy channels for plasma discharge #21 743 after 60 ms of discharge initiation. [Refer to Eq. (10).]

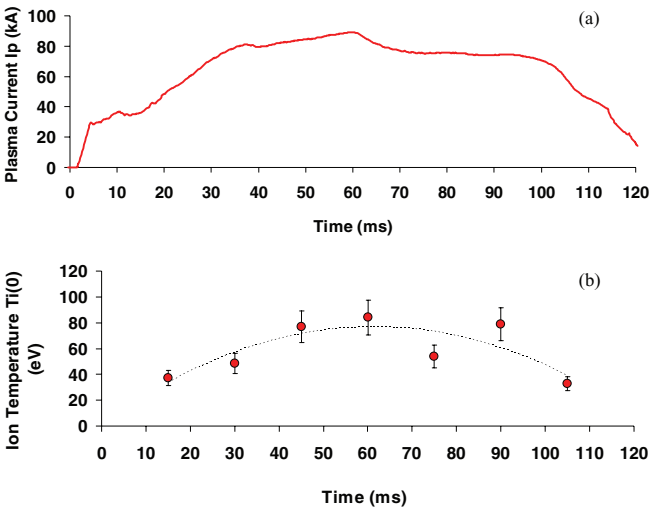

FIG. 13. For plasma dischare #21 743: (a) Plot shows evolution of plasma current with time; (b) Plot shows temporal variation of central ion temperature $T_i(0)$ during flat top of the current profile.

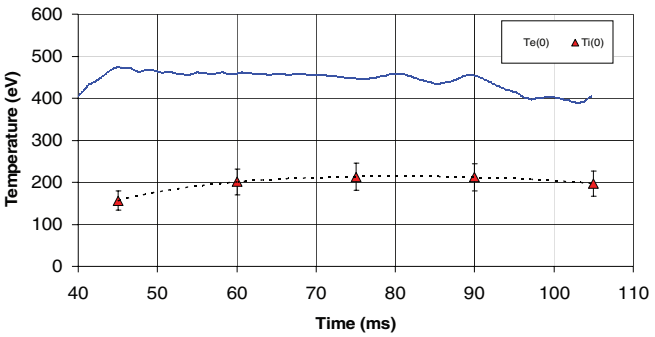

FIG. 14. Plot shows temporal variation of central electron temperature $T_e(0)$ and central ion temperature $T_i(0)$ for plasma discharge #22 738.

VIII. CONCLUSION

Passive CX-NPA is designed and developed for the ADITYA tokamak ion temperature measurement. Energy calibrations of CX-NPA were carried out using low energy ion source and the results have been found to be in a good agreement with the calculated values.

As has been found by the illustrative experimental results obtained for several neutral particle analyzers used in various tokamaks, it is a must to have a few precautionary measures for suppressing the UV radiation as they are the main source of the noise for the NPAs working with electron multiplier as ion-detectors. The upgraded NPA, with its tested UV-rejection capabilities, was found to have a fairly good signal to noise ratio (∼50) during its performance with the APPS plasma discharges.

Temporal evolution of the core ion temperature, during flat tops of the plasma current, for some APPS discharges showed the peak values of $T_i(0)$ to be ∼200 ± 30 eV which is typically 40% to 45% of the central electron temperature.

ACKNOWLEDGMENTS

Authors are very grateful to Mr. Manu Bajpai, Mr. Lavkesh T. Lachhvani, and Ms. C. Chhaya for useful discussion and technical support. Also authors are thankful to ADITYA Tokamak Operation Team, ADITYA Vacuum Team, and IPR Workshop Team for their constant help and cooperation. We express our thanks to Mr. Y. Shankara Joisa for sharing electron temperature data for a few of APPS plasma discharges.

[1]P. E. Stott, Nucl. Fusion **32**(1), 167 (1992).
[2]Equipe TFR, Nucl. Fusion **18**(5), 647 (1978).
[3]E. Haddad, C. Bélanger, B. C. Gregory, G. Abel, and H. D. Pacher, J. Appl. Phys. **69**, 1968 (1991).
[4]R. J. Fonck, R. J. Goldston, R. Kaita, and D. E. Post, Appl. Phys. Lett. **42**, 239 (1983).
[5]L. A. Artsimovich, A. M. Anashin, E. P. Gorbunov, D. P. Ivanov, M. P. Petrov, and V. S. Strelkov, Sov. Phys. JEPT **34**(2), 306–309 (1972).
[6]M. Bom, H.-D. Dicken, J. Hackpann, and J. Uhlenbusch, Plasma Phys. Control Fusion **34**, 391–396 (1993).
[7]C. B. Wharton, *A Review of Energetic Neutral Particle Plasma Diagnostics*, Laboratory of Plasma Studies, Cornell University, Ithaca, New York, USA, pp. 70–100.
[8]V. V. Afrosimov, I. P. Gladkovakii, Y. U. S. Gordeev, I. F. Kalinkerich, and N. V. Fedo rento, Sov. Phys. Tech. Phys. **5**, 1378 (1960).
[9]D. D. R. Summers, R. D. Gill, and P. E. Scott, J. Phys. E: Sci. Instrum. **11**, 1183 (1978).
[10]C. F. Barnett and J. A. Ray, Nuclear Fusion **12**, 65 (1972).
[11]H. Takeuchi, T. Matsuda, Y. Miura, M. Shiho, H. Maeda, K. Hashimoto, and K. Hayashi, Jpn. J. Appl. Phys. **22**(11), 1709–1716 (1983).
[12]H. Takeuchi, A. Funahashi, K. Takahashi, H. Shirakata, and S. Yano, Jpn. J. Appl. Phys. **16**(1), 139–147 (1977).
[13]D. Brisson, F. W. Baity, B. H. Quon, J. A. Ray, and C. F. Barnett, Rev. Sci. Instrum. **51**(04), 511 (1980).
[14]S. S. Medley, A. J. H. Donné, R. Kaita, A. I. Kislyakov, M. P. Petrov, and A. L. Roquemore, Rev. Sci. Instrum. **79**, 011101 (2008).
[15]C. J. Armentrout, G. Bramson, and R. Evanko, Rev. Sci. Instrum. **56**(11), 2101 (1985).
[16]R. Bartiromo, G. Bracco, M. Brusati, G. Grosso, S. Mantovani, B. Tilia, and V. Zanza, Rev. Sci. Instrum. **58**(5), 788 (1987).
[17]S. L. Davis, D. Mueller, and C. J. Keane, Rev. Sci. Instrum. **54**(03), 315 (1983).
[18]S. S. Medly and A. L. Roquemore, Rev. Sci. Instrum. **69**(07), 2651 (1998).

[19]Y. Nakashima, Y. Hasegawa, M. Shoji, S. Kobayashi, T. Saito, Y. Kiwamoto, T. Cho, A. Mase, M. Ichimura, A. Itakura, M. Hirata, J. Kohagura, K. Md. Islam, M. Oishi, M. Yoshikawa, T. Tamano, and K. Yatsu, Rev. Sci. Instrum. **70**(1), 849 (1999).
[20]G. Bracco, G. Betello, S. Mantovani, A. Moleti, B. Tilia, and V. Zanza, Rev. Sci. Instrum. **63**(12), 5685 (1992).
[21]T. Goto, K. Ishii, A. Nagao, Y. Goi, Y. Katsuki, N. Kikuno, N. Ishibashi, Y. Ono, M. Yamanashi, Y. Nakashima, T. Tamano, and K. Yatsu, Rev. Sci. Instrum. **70**(6), 2661 (1999).
[22]N. R. Ray, J. Phys. D: Appl. Phys. **31**, 1071–1077 (1998).
[23]D. E. Voss and S. A. Cohen, Rev. Sci. Instrum. **53**(11), 1696 (1982).
[24]S. B. Bhatt, D. Bora, B. N. Buch, C. N. Gupta, P. K. Kaw, and Y. C. Saxena, Indian J. Pure Appl. Phys. **27**, 710–742 (1989).
[25]D. Bora, Braz. J. Phys. **32**(1), 193–216 (2002).
[26]C. R. Parson and S. S. Medley, Plasma Phys. **16**, 267–273 (1974).
[27]G. A. Harrower, Rev. Sci. Instrum. **26**, 850 (1955).
[28]T. A. S. Kumar, L. M. Awasthi, C. Chhaya, H. D. Pujara, B. N. Buch, H. R. Prabhakara, and S. K. Mattoo, "Aditya charge exchange diagnostics," Technical Report IPR/TR-56/96, February 1996.
[29]Amptektron Operating Maunal for CEM Model MD-50, Revision A2, August 2005.
[30]A. N. Karpushov, B. P. Duval, C. Schlatter, V. I. Afanasyev, and F. V. Chernyshev, Rev. Sci. Instrum. **77**, 033504–033517 (2006).
[31]V. I. Afanasyev, A. Gondhalekar, P. Yu. Babenko, P. Beaumont, P. De Antonis, A. V. Detch, A. I. Kislyakov, S. S. Kozlovskij, M. I. Mironov, M. P. Petrov, S. Ya. Petrov, F. V. Tschernyshev, and C. H. Wilson, Rev. Sci. Instrum. **74**, 2338–2353 (2003).
[32]Ch. Schlatter, B. P. Duval, and A. N. Karpushov, Plasma Phys. Controlled Fusion **48**, 1765–1785 (2006).
[33]A. N. Karpushov, "Charge exchange neutral particle analysis," report (22.09.04), see https://crppwww.epfl.ch/~karpusho/Diagnostics/NPAs/DOCs/NPAonTCV.pdf.